Proceedings of the ASME 2014 International Mechanical Engineering Congress and Exposition
IMECE2014
November 14-20, 2014, Montreal, Quebec, Canada

IMECE2014-36777

EXPERIMENTAL STUDY OF INTERACTION OF TWIN LIQUID JETS ON STATIONARY AND MOVING SURFACES

M.M. Seraj
Department of Mechanical Engineering
University of British Columbia
Vancouver, B.C., V6T 1Z4, Canada
seraj@mech.ubc.ca

M.S. Gadala
Department of Mechanical Engineering
University of British Columbia
Vancouver, B.C., V6T 1Z4, Canada
gadala@mech.ubc.ca

ABSTRACT

The interaction between twin liquid jets impacts the heat transfer at interaction region. In this paper, the interaction of twin circular free surface long water jets with typical industrial parameters impinging on stationary and moving target surfaces is experimentally studied. Jets flow rate and substrate speed were systematically changed to assess radial developments of wetting front, interaction of wall jets and contours of hydraulic jumps. At stationary surface, distant jets produced thick interaction films and adjacent jets created upwash splashing thin fountains. On moving surface, same interaction types were obtained when the surface speed was slow and/or the jets flow rate is high enough to maintain the original jets interactions. However, the surface motion can principally change flow characteristics of interaction zone from strong splashing upwash fountain to oscillating nonsplashing dome-shape interaction if the surface motion has dominant effect, i.e. lower jet flow rate and/or higher plate speed. The surface speed and jet flow that determine jets interaction behaviour were experimentally found.

INTRODUCTION

Jet impingement has notable capability of cooling which has been used in various industrial cooling applications such as metal making processes [1, 2], cooling of electronic devices [3, 4], etc. Heat transfer by impinging jet especially air jet has been subject of many studies which only one jet was usually investigated. Single jet cooling can efficiently dissipate the heat at stagnation point and nearby. But, temperature increases downstream in wall zone and nonuniform heat transfer rate is imprinted over surface. Thus, local heat transfer coefficient varies radially like a bell-shape with a peak at stagnation point and decreases rapidly outward. Second maxima may occur if the flow regime changes to turbulent in wall region [5]. However in many industrial applications, heated surface is large and multiple jets have to be used to improve global cooling over entire surface by creating multi-stagnation zones. The heat transfer is not uniform over the whole surface but reasonable thermal uniformity and higher average surface heat transfer is attainable by adjusting flow rate and geometrical aspects of jets array. The improved uniformity of surface temperature is particularly desirable in industrial cooling such as steel making processes to establish proper homogeneity in steel strip properties. Spatial arrangement of jet array (in-line, staggered, and hexagonal) and geometrical parameters (jet-to-jet, jet-to-plate and jet-lines distances) greatly influence flow characteristics and heat transfer in multiple impinging jets cooling. Generally, the key factors are interjet spacing, nozzle geometry [6, 7], nozzle-to-surface distance [8-10], wall jets interaction [11, 12], and other factors such as turbulence and entrainment [13], drainage [12], and cross flow [14].

A bulk body of existing literature on multiple jets deals traditionally with wall jet interactions due to twin power lifts air jets in vertical takeoff and landing (VTOL) of aircraft. But, multiple jets also have been studied increasingly in other areas such as microjets and heat dissipation in electronic packages [for example 6, 15, 16]. Despite a great desire in industries to study the flow field and heat transfer of liquid jet interactions, little attention has been paid to multiple wall liquid jets due to free surface circular long water jets and associated upwash fountain, compared to air jets. Among the few available, Pan and Webb [8] examined the effect of jet-to-jet range ($2 \le s/d \le 8$) for two configurations of free surface jet configurations (staggered and in-line). The induced different interjet flow interactions were unimportant for local heat transfer beneath the central jet where experienced high heat extraction. However, another significant increase in heat transfer rate recorded at midway along interjet distance due to jets interaction. The position of this second maximum depends on the flow from adjacent jets and jet-to-plate spacing (*s/d*) but usually lies at equal distance from the two jets (see also [17] for air jets). Womac et al. [18] reported negligible effect of *H/d* on heat transfer for 2×2 and 3 × 3 circular jets arrays ($5 \leq H/d \leq 10$). They found heat transfer rate is higher for smaller jet space *s/d* and effect of nozzle configuration (nozzle geometry, *H/d*, *s/d*, etc.) on flow and heat transfer characteristics is more pronounced at smaller *H/d*. Slayzak et al. conducted experiments on two planar water jets [9] and two jet lines of attached circular water jets [10]. They also found enhanced heat transfer at fountain place between two planar jets or two jet-lines. Elevation of heat transfer coefficient due to jet-line interactions is comparable with counterpart at impingement region. Location of interaction zone shifts from median toward weaker jet if the jets velocities are not equal.

Ishigai et al. [19] investigated hydraulic jump (*HJ*) and interaction zone (*Int-Z*) due to laminar round water jets by measuring liquid layer thickness. The treated *HJ* and *Int-Z* are basically similar because these are both resulted from interference of two radial flows together. Indeed, thin liquid wall film interacts with thick layer at *HJ* and thin wall film with other thin wall film at *Int-Z*. They produced various types of *HJ*s ranging from stable and smooth to unstable and air entrainment by changing Froude number which defined based on film thickness. Interestingly, they observed increase and decrease in heat transfer after the *HJ*. Improved cooling was attributed to occurrence of the *HJ* before transition of flow to turbulent. Various types of interactions between two equal water jets were classified in terms of Froude number and different heat transfer characteristics at the *Int-Z* were related to this classification. Reynolds number of flow based on radius from center of jet was also found important. All these researches highlight the impact of flow field on heat transfer in *Int-Z* where presents enriched heat transfer region.

Following the studies of Ishigai et al [19] and Kate [20] on twin water free-surface round jets on stationary surface, the main regions of a typical multi-jets system can be delineated as shown in Figure 1: free jet, impingement region, inner and outer wall regions, and interaction region (*Int-Z*). The entrainment of ambient air may also occur. The free jets are conveniently called *parent jets*. Regions of free jet, impingement, and wall jet are equally defined for single jet impingement, but collision of wall jet and formation of upwash fountain in *Int-Z* are features of multi-jet systems. Outside of impingement zones, opposing liquid inner wall jets meet along interjet distance, come to be stagnant, and then deflect upward. The individual wall jets come in contact along a line in collision zone which called interaction stagnation line (or briefly *stagnation line*). Depending on strength of inner wall jets (jets momentum), a thick interaction film with no splashing or a thin sheet of upwash fountain with splattering could be shaped at *Int-Z*. Location of fountain is highly dependent on momentum ratio of opposing wall jets and it is quite sensitive to jets' conditions. Any changes in nozzle positions (e.g. jet-to-jet and jet-to-plate spaces) influence significantly the flow pattern and properties of fountain formation zone [14, 20]. Indeed, characteristics of stagnation line are strongly dependent upon relative momenta of opposing individual wall jets [15, 21]. When jets are exit from nozzles of same diameter and with same velocities, they have equal strength (momentum) and are called *equal jet* and stagnation line is straight and equidistant from each jet center everywhere. Any differences results unequal jets and the fountain shifts and leans along interjet distance toward weaker jet. For a pair of circular jets impinging vertically with *equal momentum*, location of stagnation region given as [15]

$$\frac{r_2}{r_1} = \left(\frac{V_2}{V_1}\right) \cdot \left(\frac{d_2}{d_1}\right) \tag{1}$$

where indices *1* and *2* denote the two jets, r is radial distance of stagnation line from impingement point, V is jet velocity, and d is jet diameter.

The flow field of upwash flow is rather complex and has distinct features respect to other free flows because the turbulent mixing rate is much higher than other free turbulent flows and it is remarkably three-dimensional. Although it is generally symmetric in mean characteristics but, the instantaneous velocity field is highly asymmetric with large eddies and the location of stagnation region between the two jets is displacing randomly [15, 18]. The upwash fountain is highly unsteady and very sensitive to small imbalances between the jets and may easily become unstable [16].

This paper reports the results of experiments on two round free-surface long water jets impinging on moving and nonmoving target surfaces. The velocity of moving surface and flow rate of water jets were systematically varied to inspect the flow at *Int-Z* and interaction of HJs due to two neighbor jets. The findings of the experiments on HJ due to single jet

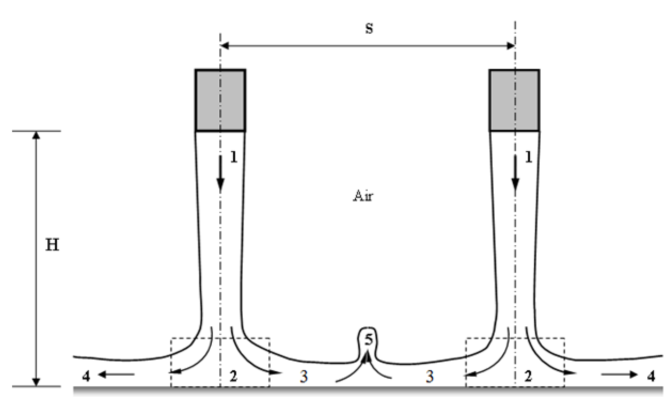

Figure 1 Twin liquid free-surface impinging jets: 1. free jet, 2. impingement zone, 3. inner wall region, 4. outer wall region, and 5. interaction region (*Int-Z*)

impinging on moving surface were presented before [22, 23]. Other series of experiments with three jets and variable nozzles height were conducted and to be reported in next publications.

EXPERIMENTAL SETUP AND PROCEDURE

The water impingement experiments were conducted in an industrial scoped run-out table (ROT) facility (Figure 2) which has following sections: furnace, acceleration zone, spray zone and deceleration zone. The main components that were used for these experiments included a hydraulic torque motor to move test bed by chain conveyor through spray section at a prescribed speed, a series of water nozzles in spray zone, and water pipe system containing upper tank, lower tank, headers, flowmeters, globe valves, etc to deliver water from upper storage tank to nozzles. The water was supplied from city line and was accumulated in upper storage tank which mounted on a rigid 6.5 m high tower. After releasing water unto test plate, water was collected in lower water storage tank to be recirculated with a centrifugal pump within the water pipe system. The water exits each nozzle at rate of up to 90 L/min. A hydraulic power unit at the end of deceleration zone drives torque motor. Two tracks provide beds for chain conveyor and prevent velocity fluctuation.

The 19 mm inner diameter tube nozzles in shape of shepherd's hook were supplied by a steel company. A test plate (1.88 × 0.508 m) is composed of two layers of MDF as base material and Plexiglas for durable finish. White painted ends used for measurement referencing. The flow rates and test plate velocities were monitored and recorded for each test. Flow rates of the nozzles were controlled by individual globe valves and test plate velocities were controlled by governing input voltage signal to proportional control valve of the hydraulic power unit. Two Sony HD camcorders were used to record the experiments at 120 frames per second and, two stand lights with variable height and lighting angle were used to provide focused illumination for filming. Further information on experimental setup can be found in [22, 23].

Prior to running the experiment, water was issued from the nozzles several minutes before starting the first test to maintain steady flow with no air bubbles at the nozzle exit. Then, the test was started from the very start of acceleration zone to allow for a steady velocity when the moving plate entered spray zone. Circular free-surface water jets were impinged normally on the test plate. Water flow development over top surface of the plate was filmed by top camera and another camera put in front end of tracks in deceleration zone. After spray zone where the experiment was recorded, deceleration zone allowed the test plate to stop unharmed. Due to short length of deceleration zone, experiments faster than 1.5 m/s were unable to be conducted in a safe fashion. Furnace was not utilized in any of these experiments and the experiments were run at room temperature. Same test plate is used for stationary test.

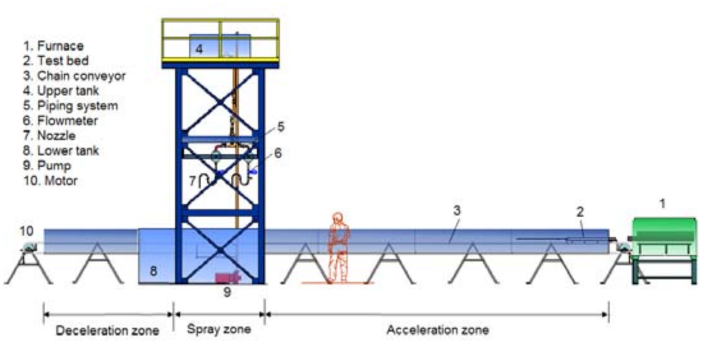

Figure 2 Schematic of pilot scale run-out table apparatus

A set of moving experiment is represented by a jet flow rate Q (or jet Re number) and a test surface velocity V_p. In these experiments, jets Q varied from 10 to 30 L/min and the test plate V_p ranged from 0.6 to 1.5 m/s. The twin nozzles was lined up in an inline array and separated by a distance of 203.2 mm ($s/d \cong 10.7$) at same horizon. The vertical distance between the nozzles and the test plate was kept at $H = 1.5$ m. The experiments were conducted with industrial scale parameters. In mill conditions, inline arrays of round nozzles stand 1-2 m above strip, nozzle flow rate is up to 90 *L/min* and strip speed is 2.5 - 15 m/s [2, 24]. Table 1 summarizes 18 sets of moving experiments and also some more for nonmoving experiments. Jet Reynolds number Re is defined based on jet exit velocity V at nozzle outlet and nozzle diameter d as $Re = \rho Vd/\mu$. The studied jet Re numbers were relatively high (table 1) and, in turn, the water jets were turbulent particularly for higher jet flow rates at exit of the nozzles. Moreover, the jets were accelerated and contracted significantly after discharging due to gravity effect within large distances between nozzle and target surface (H/d = 79) [22, 25]. Accordingly, jets velocity at impingement surface V_{imp} is increased substantially respect to the ones at nozzle outlet and resulted impingement Reynolds number ($Re_{imp} = \rho V_{imp} d_{imp}/\mu$) are much higher than jets Re at nozzle exit (table 1). Therefore, intensified turbulent incoming jet was impinged on the target surface and consequently influenced the wall jets and jets interaction over the surface.

Each set of moving experiments was usually repeated 10 time and more to ensure that accurate and repeatable experimental results is documented. Great care was taken throughout each repeated test to guarantee that nearly identical

Table 1 Experimental parameters for two nozzles tests

V_p (m/s)	Q (L/min)	V (m/s)	Re	V_{imp} (m/s)	Re_{imp}
0, 0.6, 1.0, 1.5	10	0.588	11,126	5.457	33,890
	15	0.882	16,690	5.496	41,666
	22	1.293	24,478	5.577	50,832
	30	1.763	33,380	5.704	60,032

conditions were maintained for the jets and plate motion in every set. But, jet flow rate *Q* and plate velocity *Vp* were not perfectly constant during each test. Indeed, some variations were unavoidable and beyond control. For example, the seemingly identical nozzles did not deliver the same flow rates although flow meters were carefully and frequently checked and regulated. Therefore for each set of experiments, the time average of nozzle flow rate and the time average of plate velocity and their variation during each repetition were calculated [26]. The fluctuations in plate speed were usually around 10 percent or less but it was higher for 0.6 m/s test set. A slower moving test plate made it harder to establish a steady plate motion during the test because the starting speed had to be higher than 0.6 m/s to overcome static friction. In addition, nozzle flow rates were not exactly equal during the tests. However, the inequalities among nozzles did not exceed 4 percent and variations of flow rate were, generally, limited to below 5 percent. Higher variation was seen for 10 *L/min* tests. Accordingly, the highest flow rate inequality and plate speed unsteadiness occurred in the set of 10 L/min and 0.6 m/s experiments.

DATA PROCESSNG

The films taken from the experiments were assessed frame-by-frame using Matrox Inspector image processing software. The frames were saved by Sony's Picture Motion Browser software. A wire mesh was sited between the nozzles and the test plate for mean of scaling the frames taken from the recorded films. The wire mesh consisted of 0.0254 m squares and was picked up by the top high speed camcorder which facing downward normal to the mesh and the test plate. Using the reference squares, points on the wire mesh were used for calibration by image processing software. Variable plate speed and jet flow rates and inequality between nozzle deliveries influenced jets interaction and increased unsteadiness at the *Int-Z*. Considering high degree of unsteadiness of upwash flow in *Int-Z*, a large number of frames from every film is required to explore the flow at *Int-Z* and to precisely gauge effect of plate motion. The scope of this research is confined to investigation of overall effects of test plate motion on jets interaction and as such, 4 frames per each film were usually selected at the most different situations to do measurements for upwash interactive flow (e.g., shape, place, etc). Collected data from the 4 frames were used to represent place and shape of *Int-Z* for the test. Similarly, collected data from all repetitions were combined to determine final representative for each set. These steps in data processing have been described in more details in [26]. It is believed that the collected data from those frames represent, in general, the boundaries for size and place of *Int-Z* over impingement surface during each test set and is enough to inspect effect of test plate motion. However, these results do not reflect instantaneous behavior of interfering wall jets at every instant during the experiments.

Despite all the care taken during the experiments to ensure symmetry in flow and due to inevitable imperfections, interference region and upwash flow sometimes displayed a tendency to incline toward the weaker jet at that moment and the stagnation line was not a straight line. This verifies high sensitivity of fountain to asymmetries in jets conditions such as slight uncontrollable inequality in flow rates among the nozzles in jets array. This was also reported by other researchers [e.g., 15-16]. Moreover, impingement flow in wall region was turbulent ($33,000 < Re_{imp} < 61,000$) with a wavy surface; surface disturbances from parent incoming jets were transferred to impingement water flows and perturbed the wall jets surfaces [23]. This disturbed wall jet flows before collision in the experiments and triggered asymmetry and unsteadiness at *Int-Z*.

EXPERIMENTS OF TWIN JETS ON STATIONARY TARGET SURFACE

Interaction of circular hydraulic jumps (*CHJ*s) is studied through our twin jets tests on fixed test plate surface. After impingement of each water jet over test surface, a *CHJ* is formed and *CHJs* interference is happened in *Int-Z* due to collision of twin inner wall jets. Kate et al [20] investigated *CHJ*s interaction due to twin water jets impinging on stationary surface. They classified the jets interactions to *Far-distant*, *Distant*, and *Adjacent* jets. For a given jet *Q*, strong *HJ*s interaction and resulted upwash fountain is created by close neighboring jets (adjacent jet) and weak *CHJ*s interaction with no splattering is obtained by larger inter-jet distances (distant jets). On other hand, higher jets flow rate strengthen *CHJ*s interaction for a given jets space (*s/d*). In turn, flow structure and interaction type at *Int-Z* are controlled by both jet flow rate *Q* and nozzles distance *s/d* on stationary surface. In our tests, different flow rate for long turbulent jets was examined to inspect its effects on interaction flow on stationary surfaces.

Figures 3 shows the sample images of *CHJ*s interference from top view (taken by top camera) and front view (taken by front camera) for different jet flow rates due to twin jets. Various interaction films were happened depends to the jets *Q*. The inner opposite wall jets were spreading radially, touching each other and producing two types of interactions. As shown in Figure 3a for 15 *L/min* jets (and similarly for 10 *L/min* jets), a dome-shape thick film took placed with almost no splashing because *lower flow rate jets* made smaller *CHJ*s giving less interference of small two circles and then weak *HJ*s interaction. However as shown in Figure 3b for 30 *L/min* jets (and for 22 *L/min* jets similarly), a thin upwash fountain happened because the *higher flow rate jets* produced larger *CHJ*s giving strong interaction of *HJ*s. Therefore, *higher jet Q* will intensify the *HJ*s interference. The size of *CHJ*s was large for higher jets *Q*s which were not captured by the camera. Both distant and adjacent jets interactions were obtain and observed in our tests by various jets *Q*. The stagnation lines during these tests were not perfectly straight and displacing at inter-jet space according to the variability of jets flow rate and movement of impingement points. This caused oscillating thin and thick interference films in *Int-Z*.

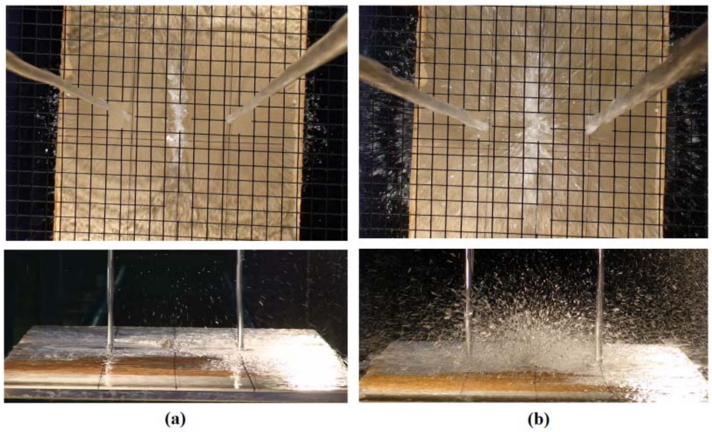

Figure 3 Hydraulic jumps interaction on due to twin jets (*H/d* =79, s/d ≅ 10.7) impinging on stationary surface (a) Q = 15 *L/min* (b) Q = 30 *L/min*

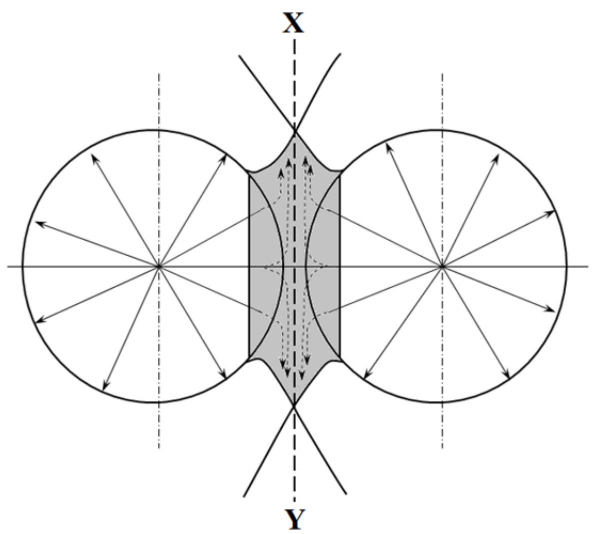

Figure 4 Schematic of two HJs interaction due to two liquid adjacent jets impinging on stationary surface

Figure 4 schematically depicts the interaction of two *CHJ*s (two circles) from impingement of twin liquid jets. The lines inside the circles represent radial wall streamlines originated from each impingement point (circle center) which colliding along stagnation line XY at the (gray region) and exit it from both upper and lower sides of *Int-Z*. The dashed lines illustrate returning flow from upside and downside of the *Int-Z*. The type of *CHJ*s interference depends to the size of the two circles and as shown in Figure 3, it is governed by jets flow rate Q in our tests. Although the two neighboring *CHJ*s interfere at the *Int-Z* but their identities and shapes (circles) are preserved because the *CHJ*s interference of the inner wall jets occurred only at portions of the jumps in the *Int-Z* and so the *CHJ*s interaction is depend on angular direction of radial streams. Highest interference is seen along inter-jet line and it is decaying as going outward along the stagnation line. As such, the water thickness along line XY is decreasing outward as well [20]. Dependency on angular direction signifies the complexity involving in circular liquid jets (*CHJ*s) interaction and indicates three-dimensionality of flow at *Int-Z*.

EXPERIMENTS OF TWIN JETS ON MOVING TARGET SURFACE

The two jets in the experiments setup are distant jets (s/d = 10.7). Figures 5 and 6 illustrate sample images from development of impingement flow and interaction of twin jets over moving test surface. These image frames were extracted from films of experiment from set of 10 L/min and 1.5 m/s (Figure 5) and set of 22 L/min and 1 m/s (Figure 6). Parts (a) of the figures were taken by top camera and parts (b) were taken by front camera from same tests. As shown, the front end moving plate hit the jets columns and the impingements started. Initially, the flow from each jet was spreading individually over moving surface similar to single jet impingement. Thereafter soon, inner wall jets met at test surface centerline and striking was launched. At higher jets Qs tests, interactions were observed faster. On moving impingement surface, thin radial wall jets were not allowed to flow freely forward and restricted by surface motion and thick wetting front (as *HJ*) resulted similar to what observed for *HJ* (wetting front) due to single jet experiments [23]. Moving test surface influence radial progress of circular wetted zone in all direction and alter circular *HJ*s at wetting front on fixed surface into noncircular contours on moving surface. However, the two *HJ*s interacted similar to twin jets tests on stationary surface (Figure 3) at the beginning, and thick dome-shape interaction film (figure 5) or thin upwash splashing fountain (Figure 6) took place according to jets Q over moving surface. The place of *Int*-Z, in general, was variable with wavy stagnation line but confined around surface centerline. The round waves over free-surfaces of wall jets, which originated from surface disturbances along jets column, also agitated upwash unsteadiness.

Figure 5 shows jets of lowest Q impinging on fastest moving test plate in the present tests setup (highest velocity ratio V_p/V = 2.55). As shown, whenever effect of plate motion is promoted a double curved front of wetted area created above the two impingement points. Single curve wetting front was obtained at single jet tests on a moving plate [23]. On other hand, as shown in Figure 6 for higher jets Q and lower surface V_p test (lower velocity ratio = 0.77), an upwash high- rise fountain generated with noticeable splattering. The returning flow from the *Int*-Z combined with accumulated water ahead of the *Int*-Z and pushed forward locally the double wetting front to ahead. Then, impingement water sheet covered larger area over moving surface. This was also observed at the experiments with single jet at higher jet Qs (30 and 45 *L/min*) impinging on slow moving plate [23]. For twin jet experiments, however, the wetted front grew and swelled around plate center line and pool of impingement water was created centrally (Figure 6).

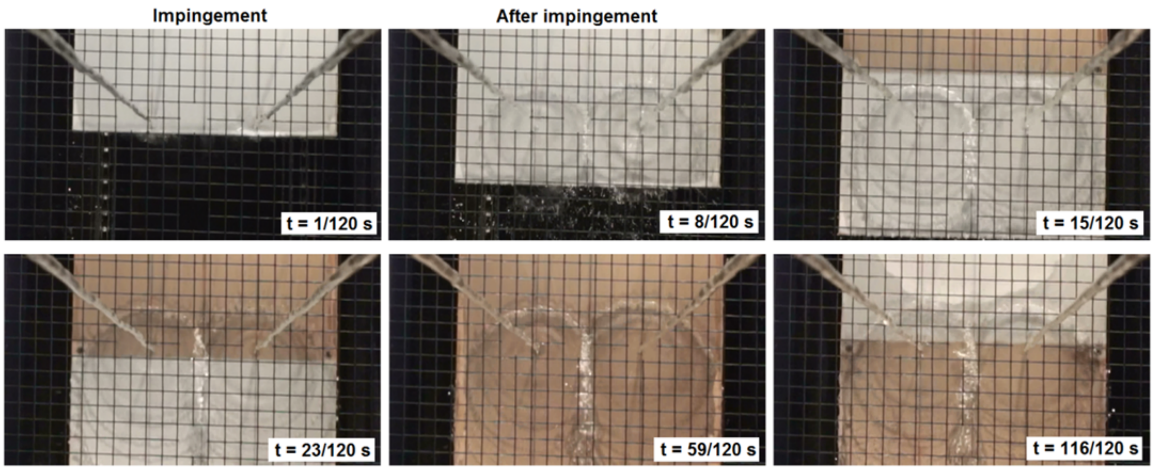

(a)

(b)

Figure 5 Impingement flow development and interaction of twin jets on moving surface, Q = 10 L/min, V_p =1.5 m/s
(a) top View (b) front View

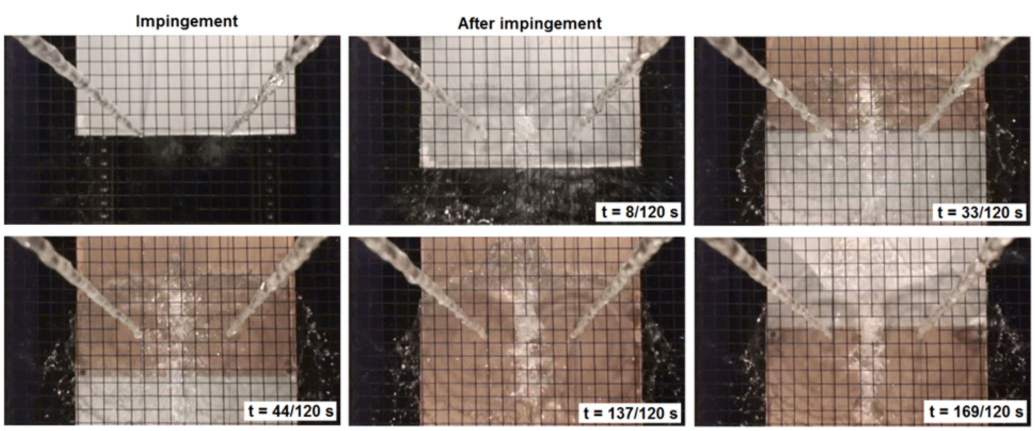

(a)

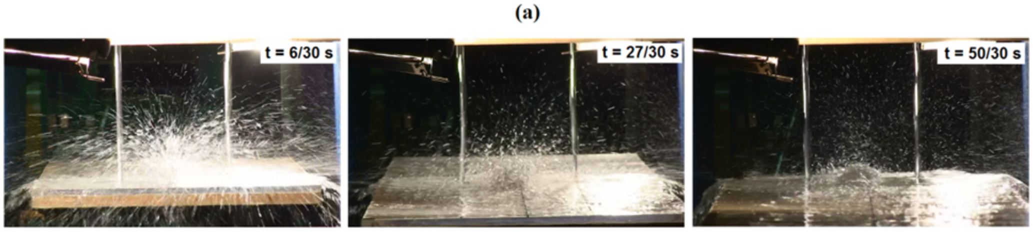

(b)

Figure 6 Impingement flow development and interaction of twin jets on moving surface, Q = 22 L/min, V_p =1.0 m/s
(a) top View (b) front View

During these experiments, thick interaction films were developing as moving surface passed beneath jets but it usually established at second half of plate surface. Thereafter, the established interactions are shown in next figures. Effect of test plate surface motion at different velocities on interactions of *Q*= 10 and 15 *L/min* twin jets illustrate in Figure 7. For each jet *Q*, dome-shape interaction water layer was higher stand up and thinner on faster moving surface. For each *Vp*, thick interaction film was wider and higher stand up for stronger jets (15 *L/min*). On non-moving surface, interaction film freely drained water upside and downside along stagnation line in both directions. However, motion of impingement surface restricted wetting front ahead of *Int-Z* and increased complexity there. As demonstrated in Figure 7, returning flow from *Int*-Z interfered with radial inner wall streams and it could cause displacing of *HJ* fronts ahead of *Int-Z* if moving plate is not enough influential such as *Vp* = 0.6 *m/s* and/or higher jet *Q* (15 *L/min*) tests. Consequently, returning flow from *Int-Z* could push successfully wetting front outward and made a thick pool of water ahead of *Int*-Z by joining with radial streams from two wall jets at related angular position above the *Int-Z*. As such, wetting front detached from individual *HJ* fronts locally above *Int*-Z and produced larger wetting area centrally over moving surface. At same *Vp*, a bigger local central enlargement was detected at 15 *L/min* jets tests. Faster moving plates (*Vp* = 1.0 *m/s*) presented smaller bumps ahead of *Int-Z*. No local swelling along wetting front had occurred at 10 *L/min*, 1.5 *m/s* test set and two complete noncircular colliding *HJ*s had occurred above impingement points which formed a double curved wetting front at moving surface (Figure 7a). But, small bulge eventually occurred ahead of *Int-Z* at 15 *L/min*, 1.5 m/s test set. Although test plate motion limited exit of returning flow upstream of *Int-Z* but it facilitated flow drainage to *Int*-Z downstream. In turn, exiting flow spread over surface while diverting from centerline of *Int-Z* (see figure 5b for example).

This is interesting to examine if the double curved wetting front by twin jets can be reproduced from combination of single jets tests. Figure 8 shows wetting fronts from single (N = 1) and twin jets (N = 2) experiments of *Q* = 10 *L/min* and *Vp* = 1.5 *m/s* set. A double curved wetting front is made from measured data of twin jets tests but the two single curve wetting fronts are obtained from measured data of single jet test [23]. The shown curves are fitted curves to measured data at the experiments. These tests series (N = 1, 2) have highest velocity ratio among the present tests (V_p/V_j = 2.55). Impingement point of single *HJ* was originally at surface centerline but it was shifted $-s/2$ and $+s/2$ along jets centerline at two sides to reproduce two virtual impingement points. In this way, two offset interacting single *HJ*s are created artificially from measured data of single jet tests to be compare with the real double curve wetting front at the twin jets test. In addition of wetting fronts, *Int-Z* was also measured in twin jets and depicted in figure 8. As shown, the intersection point of two offset single curves (N = 1) is at stagnation line and it is at the vicinity of where the interaction of *HJ*s in twin jets test was really started. It has to be noted that variations of jets *Q* were not identical during these two tests sets and also impingement points of twin jets were not coincident with shifted impingement points of the curves from single nozzle tests. As illustrated, the wetting front from twin jets can be assembled reasonably well from the two individual interacting *HJ*s which obtained from single jet and it also can represent well the *Int-Z*. This is true as along as the ratio of impingement surface speed to jet velocity is high which a central enlargement is not occurred ahead of *Int-Z*. Also, the radius of *HJ* for each of all tests in the set of *Q* = 10 and 15 *L/min* were measured and compared with radius of *HJ* from single impinging jets on a moving plate for same jet *Q* and good agreement were found [22, 23]. Thus, single jet experiment on a moving surface can be used as an approximate for wetting front due to twin jets.

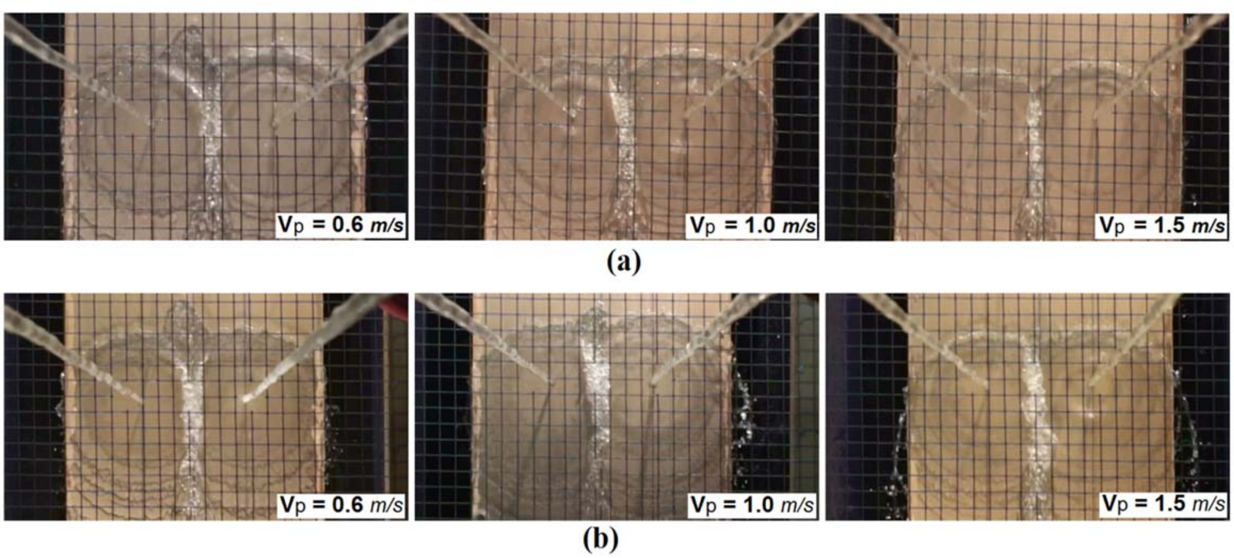

Figure 7 Twin jets interaction on moving surface at various velocities, (a) *Q* = 10 L/min, (b) *Q* = 15 L/min

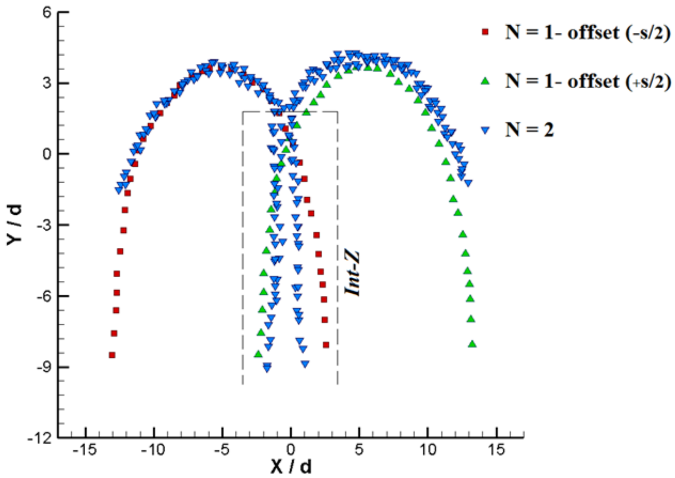

Figure 8 Measured wetting fronts and *Int-Z*, Q = 10 *L/min*, V_p = 1.5 *m/s*

Experiments with higher twin jets flow rates of 22 and 30 *L/min* which impinging on moving surface at different velocities are illustrated in Figures 9 and 10, respectively. At the beginning, upwash fountain was created with a high splashing but it gradually decreased after evolution of wetting front over the moving surface. Larger and thicker pool of water and faster growing central bulge ahead of *Int-Z* were observed as a result of stronger radial streams and more returning flow exiting the *Int-Z*. The intensive splattering was gradually fading after the highrise thin upwash fountain progressed and maintained over the moving surface. An interesting feature observed during 22 *L/min* jets impinging on fast moving surface. If effect of surface motion is dominated (high velocity ratio due to higher plate speeds), the thin upwash fountain started transition to thick liquid layer with less splashing from upside end of the *Int-Z*. Finally, the splashing reduced tremendously and a high stand up oscillating dome-shape blanket of liquid was developed entirely at the *Int-Z* (Figures 6 and 9) similar to interference at lower jets *Q*s tests (Figure 5, 7). Faster conversion was detected at higher V_p where wetting front is closer to the *Int-Z*. For V_p = 0.6 m/s tests, transfer in the interaction flow was retarded and did not extend fully through *Int-Z*. During 30 *L/min* tests sets, the fountain was stronger and the wetting front was more distant from the *Int-Z* due to collision of high strength wall streams, and, in turn, the splashing fountain was more intensified and persistent (Figure 10). In fact, the water eruption from *Int-Z* was decreased but was not diminished as observed in the Q = 22 *L/min* tests (Figure 9). Careful assessment of the films revealed that the shift in the *Int-Z* was initiated at upside end with reduced splashing and thicker interaction sheet over fast moving surface (V_p = 1, 1.5 m/s) where the wetting front was closer to the *Int-Z* (Figure 9a). However, the transformation was not settle down and only occurred partially because the effect of surface moving is least for 30 L/min tests (lower velocity ratio = 0.85) comparable to the other jets *Q*s tests and, then, the fountain flow structure are mostly controlled by parent jet conditions during these tests. Another interesting feature for these jets *Q*s sets is *HJ* confinement due to pool of water and wetting front. This restriction effect is similar to controlling effect of a rim around test plate border on size of *CHJ* through height of liquid layer after the jump. In turn, development of *HJ*s was suppressed over moving plate and then, they were detectable for 30 *L/min* set in contrast with their large size over stationary surface at same jets *Q* which was not captured by the camera (figure 3). For high jets *Q*s (22 and 30 *L/min*), wetting fronts detached from *HJ*s around central line of moving surface ahead of *Int-Z*. To sum up for these high *Q*s jets test sets, plate motion

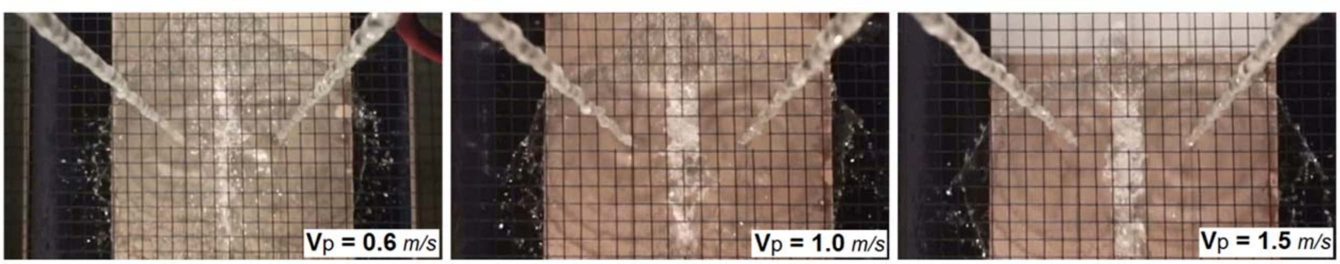

(a)

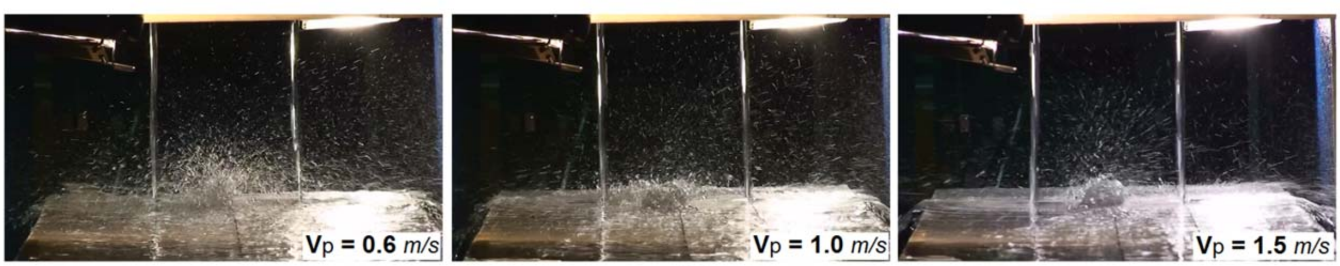

(b)

Figure 9 Twin jets interaction on moving surface at different velocities, Q = 22 L/min (a) top View (b) front View

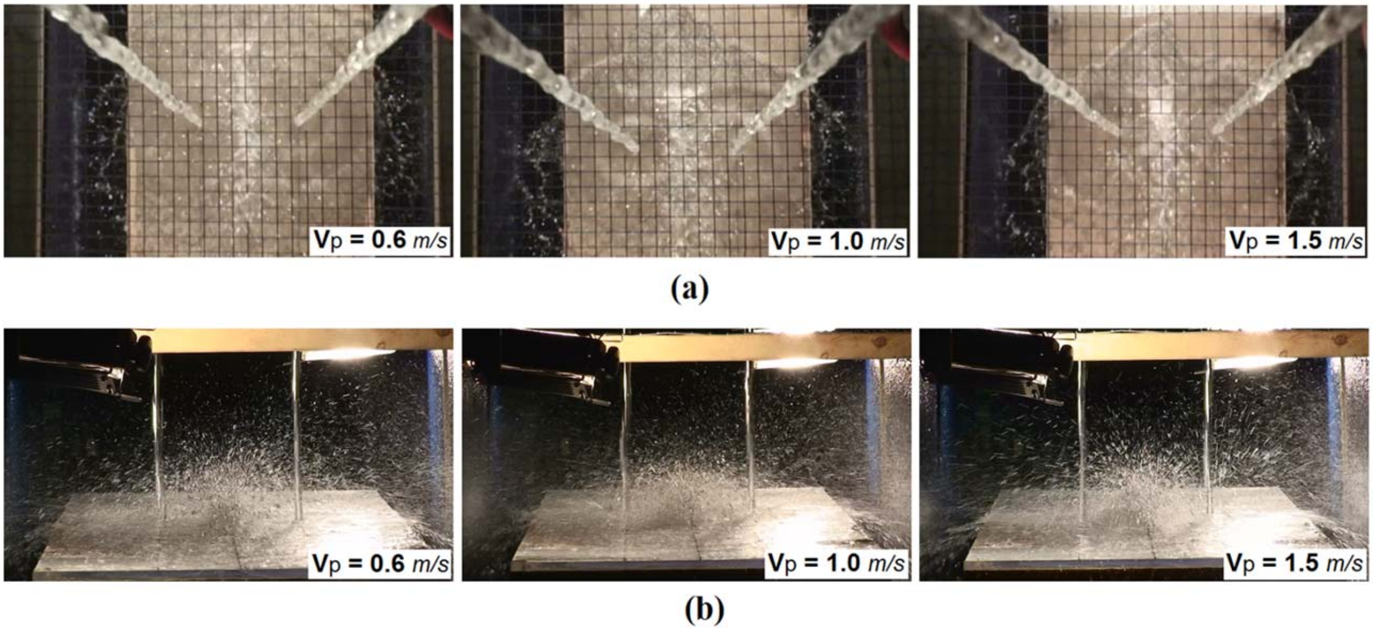

Figure 10 Twin jets interaction on moving surface at different velocities, Q = 30 L/min (a) top View (b) front View

could influence both *HJ* size and shape and jets interaction type simultaneously through the proximity of wetting front to *Int-Z*. To our best knowledge, the essential change in type of flow characteristic and structure from strong splashing thin fountain to thick interaction film at the *Int-Z* between twin water long jets by moving impingement surface was not reported in the literature.

The flow regimes in *Int-Z* for variety of plate speed and jet flow rate is mapped in figure 11 as two distinct modes of oscillating dome shape and splashing fountain. As shown, lower flow rate jets impinging on faster moving surface

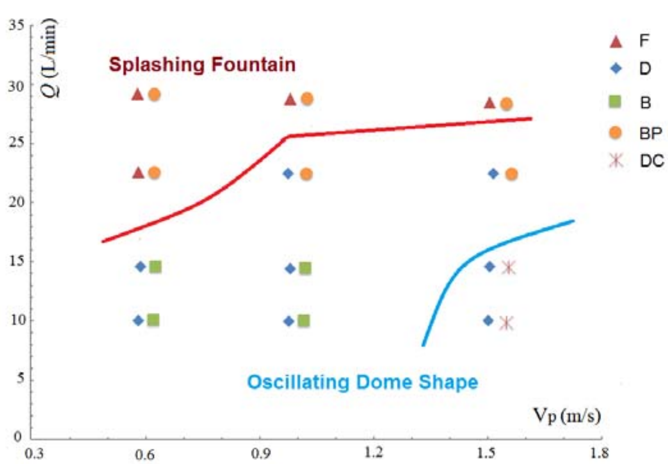

Figure 11 Flow regime map in Int-Z due to twin jet interaction (F = fountain, D = dome-shape, B = interface bump, BP = bump and pool, DC = fully double curve)

produce nonsplashing dome shape interaction and upwash splattering is resulted from collision of high flow rate jet. Exceptionally, only 22 L/min jets results oscillating dome-shape interaction on fast moving plate (Vp = 1.5 m/s).

Figure 12 depicts schematically the top view of interaction of two *HJ*s due to impinging of twin liquid jets on a moving surface V_p. Dashed circles illustrate the *HJ*s and dashed lines illustrate radial flows over non-moving impingement surface for same jet Q similar to Figure 4. Solid bold curves represent the front of the jumps over moving surface and solid lines show radial streams emitted from two impingement points. The radial stream lines were rotated downward by moving surface. In fact, surface motion distorts circular contour of the *HJ*s and shapes them to noncircular form. The two noncircular jumps intersect but their identities are conserved. This is also observed for single jet tests impinging on moving surface [23]. Again, angular direction is important here. Influence of surface motion is not the same at above impingement points where surface motion opposes radial flows and at below impingement points where radial streams are assisted by surface motion. Therefore, significance of surface motion for impingement flow and the *HJ*s contours is dependent on angular direction. The effect of plate motion can be considered as a superposing the shear effect beneath interaction flow at *Int-Z* and beneath wall jets over surface which induces flow flux in direction of motion (i.e. Couette flow). The flow at *Int-Z* on moving surface is more complicated than *Int-Z* over stationary surface (figure 4) where angular direction is only important at *Int-Z* but not on rest of the *HJ* contour which kept circular. Indeed, conditions on

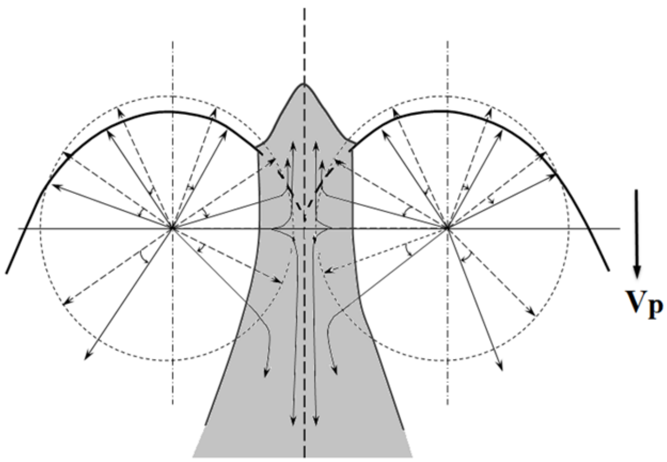

Figure 12 Schematic of HJs interference on a moving surface

outflows from upstream and downstream of *Int-Z* are identical on stationary surface but substrate motion produces different boundary conditions at the two outlets of *Int*-Z. The returning flow is drained downstream freely which is helped by surface motion but outflow to ahead of *Int-Z* is confined due to presence of wetting front and pool of water. Thus, the transition from thin upwash to thick film started from upside of *Int*-Z where exiting flow push the wetting front forward to lift its limiting effect on drainage ahead of *Int*-Z. A size of local enlargement ahead of *Int-Z* is controlled by surface motion and jets *Q*. Velocity ratio of test surface to jet can be used as controlling parameter but jet *Q* is important individually. At higher velocity ratio, smaller central enlargement is formed there. Principally, motion of impingement surface with enough high speed ($V_p \geq 1$ m/s) can prevent formation of central bump and can result happening of colliding noncircular *HJ*s (thick dashed lines shown in Figure 12) over fast moving surface which bounding with a double curved noncircular wetting front. This is true except for highest jet *Q* (30 *L/min*) test sets which highlights importance of jet *Q* as well. Even with highest plate speed (V_p = 1.5 *m/s*) in 30 *L/min* jets, excessive amount of fluid generated pool of water and counteracted confinement resistance due to surface motion.

The impact of flow structure conversion at *Int-Z* on heat transfer is of especial interests for industries used liquid jet impingement cooling. In ROT scale, the strip is moving much faster and stronger splashing fountains due to closed jets in jet-line are occurred which potentially waste considerable amount of coolant and reduce cooling efficiency. Although present experiments were performed with plate speed limitations at the pilot scale ROT apparatus but even these tests demonstrate the effect of substrate motion on reducing splashing and altering the mode of jets interaction to nonsplashing type. Therefore as illustrated in this experimental study, fast moving strip in expected to entrain greatly coolant impingement flow and impact substantially or diminish the splattering. Minimum strip speed that required converting the fountain interaction to nonsplashing interaction in mill condition should be investigated. Furthermore, the effect of addition of heat transfer on development of wall jets interaction and on formation of wetting front over moving substrate should be explored in pilot scale first. More importantly, effect of heated impingement surface on jets interaction type and associated heat transfer characteristics for each type of interaction should be investigated.

SUMMARY AND CONCLUSION

In this paper, the interactions of free-surface circular liquid jets were studied experimentally by two in-line jets configuration. Depending on jet *Q* for the specified nozzles spacing, thick interaction films or upwash splashing fountains obtained at stationary test plate according to strength of parent jets. Influence of impingement surface motion was studied for a range of jet *Q* and plate surface V_p. When surface motion was slow or jets interactions were intensified due to high jets *Q*, interaction types on moving surface were same as on non-moving surface. However, surface motion can essentially change *Int*-Z flow characteristics if its effect was enhanced enough (i.e., lower jets *Q* and/or higher V_p). The wetting front proximity to *Int*-Z is important. The interaction flow identity transforms from strong splashing upwash fountain to weak nonsplashing interaction dome-shape region when wetting front is near to *Int*-Z. In addition to the effect on *Int*-Z, it was shown that surface motion can influence contour of individual *HJ* due to each jet and also this is the wetting front that controls *HJ* radius as well.

It experimentally demonstrates that fast moving impingement surface can conquer splashing fountain in *Int*-Z even for strong water jets (high jet *Q*, e.g. 22 *L/min*) for $V_p \geq 1$ m/s. Nonetheless, volume of spreading water is also a key parameter (e.g. for 30 *L/min* jets). The change in hydrodynamics of interaction liquid wall flow on a moving surface needs more studies particularly for qualitative investigation of changes in velocity and pressure fields and related turbulent parameters. Moreover, change is heat transfer and cooling efficiency at *Int*-Z due to alteration of flow structure should be explored and is of interest for industries.

ACKNOWLEDGMENT
This research was supported from the Qatar National Research Foundation (QNRF), Qatar.

REFERENCES

[1] R. Viskanta, F.P. Incropera, Quenching with liquid jet impingement, In: Tanasawa I., N. Lior, (eds): Heat and Mass Transfer in Materials Processing, Hemisphere Publishing, New York, 1992 pp. 455-476.
[2] G.A. Franco, , M.A. Wells, , M. Militzer, Effect of nozzle configuration on cooling of a hot moving steel plate, Canadian Metallurgical Quarterly, 48(2009), 197-206.
[3] M.K. Sung, I. Mudawar, Single-phase and two-phase heat transfer characteristics of low temperature hybrid micro-

channel/micro-jet impingement cooling module, Int Heat Mass Transfer, 51(2008), 3882 -3895.
[4] S. Narumanchi, A. Troshko, D. Bharathan, and V. Hassani, Numerical simulations of nucleate boiling in impinging jets: Applications in power electronics cooling, Int Heat Mass Transfer, 51(2008), 1-12.
[5] Liu, X., Lienhard, J. H. V., and Lombara, J. S., Convective Heat Transfer by Impingement of Circular Liquid Jets, *J. Heat Transfer*, Vol. 113, pp. 571-582, 1991
[6] Whelan, B. P., Robinson, A. J, Nozzle Geometry Effects in Liquid Jet Array Impingement, *Applied Thermal Eng*, Vol. 29, pp. 2211-2221, 2009.
[7] Barata, J. M. M., Sousa, N. M. S., Silva, A. R. R., Meireles, P. M. S., Flow Characteristics of Twin Impinging Jets, *47th AIAA Aerospace Sciences Meeting*, 2009.
[8] Pan, Y., Webb, B. W., Heat Transfer Characteristics of Arrays of Free-Surface Liquid Jets, *J. Heat Transfer*, Vol. 117, pp. 878-884, 1995
[9] Slayzak, S. J., Viskanta, R., Incropera, F. P., Effect of Interactions between adjacent Free Surface Planar Jets on Local Heat Transfer from the Impingement surface, *Int. J. Heat Mass Trans,* Vol. 37, pp. 269-282, 1994.
[10] Slayzak, S. J., Viskanta, R., Incropera, F. P., Effect of Interactions between Adjoining Rows of Circular, Free Surface Jets on Local Heat Transfer from the Impingement surface, *Int. J. Heat Mass Trans,* Vol. 116, pp. 88-95, 1994.
[11] Abdel-Fattah, A., Numerical and Experimental Study of Turbulent Impinging Twin-jet Flow, *Exp Thermal Fluid Science*, Vol. 31 pp. 1061-1072, 2007.
[12] Garrett, K., Webb, B. W., The Effect of Drainage Configuration on Heat Transfer under an Impinging Liquid Jet Array, *J. Heat Transfer*, Vol. 121, pp. 803-811, 1999
[13] Geers, L. F. G., Hanjalic, K., Tummers, M. J., Wall Imprint of Turbulent Structures and Heat Transfer in Multiple Impinging Jet Arrays, *J. Fluid Mech*., Vol. 546, pp. 255-284, 2006.
[14] Barata, J. M. M, Fountain Flows Produced by Multiple Impinging Jets in a Crossflow, *AIAA J*., Vol. 34, pp. 2523-2530, 1996
[15] Siclari, M. J., Hill Jr., W. G. Jenkins, R. C., Stagnation Line and Upwash Formation of Two Impinging Jets, *AIAA J*., Vol. 19, pp. 1286-1293, 1981.
[16] Cabrita, P. M., Saddington, A. J., Knowles, K., PIV Measurements in a Twin-Jet STOVL Fountain Flow, *Aeronaut. J*., Vol. 109, pp. 439-449, 2005.
[17] Hoberg, T. B., Onstad, A. J., Eaton, J. K., Heat Transfer Measurements for Jet Impingement Arrays with Local Extraction, *Int. J. Heat Fluid Flow*, Vol. 31, pp. 460-467, 2010.
[18] Womac, D.J., Incropera, F.P., Ramadhyani, S., Correlating Equations for Impingement Cooling of Small Heat Sources with Multiple Circular Liquid Jets, *J. Heat Transfer*, Vol. 116, pp. 482-486, 1994.
[19] Ishigai, S., Nakanishi, S., Mizunao, M., Imamura, T., Heat Transfer of the Impinging Round Water Jet in the Interference Zone of Film Flowing Along the Wall, *Bull. JSME*, Vol. 20, pp. 85-92, 1977.
[20] Kate, R.P., Das, P.K., and Chakraborty, S., An Experimental Investigation on the Interaction of Hydraulic Jumps Formed by Two Normal Impinging Circular Liquid Jets, J. Fluid Mech., Vol. 590, pp. 355-380, 2007.
[21] Saripalli, K. R., Laser Doppler Velocimeter Measurements in a 3-D Impinging Twin-jet Fountain Flow, AIAA, *AHS, and ASEE, Aircraft Design Systems and Operations Meeting*, Colorado, USA, 1985.
[22] M. M. Seraj, M. S. Gadala, Experimental investigation of wetted zone of an impinging circular water jet on a moving surface, ASME Int. Mech. Eng Cong Exposition, 2010, IMECE-39399, Vancouver, Canada.
[23] M. M. Seraj, M. S. Gadala, Noncircular Hydraulic Jump on a Moving Surface due to an Impinging Circular Free Surface Jet of Water, *Steel Research Int*., 2012, DOI: 10.1002/srin.201100339
[24] Hernandez, V.H., Modeling of the Thermal Evolution of Steel Strip Cooled in the
Hot Rolling Runout Table, PhD Thesis, University of British Columbia, BC, 1999.
[25] M. M. Seraj, M. S. Gadala, Numerical investigation of impingement flow due to a long axisymmetric water jet, ASME Int. Mech. Eng Cong Exposition, 2011, IMECE2011-63185**,** Denver, USA
[26] M.M. Seraj, Hydrodynamics of circular free-surface long water jets in industrial metal cooling, PhD Thesis, University of British Columbia, Canada, 2011

